




## Pomelo (*Citrus grandis* (L.) Osbeck) sponge layers as a potential source of soluble dietary fiber: Evaluation of its physicochemical, structural and functional properties

Follow this and additional works at: <https://www.jfda-online.com/journal>

 Part of the [Food Science Commons](#), [Medicinal Chemistry and Pharmaceutics Commons](#), [Pharmacology Commons](#), and the [Toxicology Commons](#)



This work is licensed under a [Creative Commons Attribution-Noncommercial-No Derivative Works 4.0 License](#).

### Recommended Citation

Chen, Xiaowei; Chen, Jiajia; Peng, Jian; Yu, Yuanshan; Wu, Jijun; Wen, Jing; Kang, Zhiying; Wang, Yanhui; Xu, Yujuan; and Li, Lu (2024) "Pomelo (*Citrus grandis* (L.) Osbeck) sponge layers as a potential source of soluble dietary fiber: Evaluation of its physicochemical, structural and functional properties," *Journal of Food and Drug Analysis*: Vol. 32 : Iss. 1 , Article 3.

Available at: <https://doi.org/10.38212/2224-6614.3489>

This Original Article is brought to you for free and open access by Journal of Food and Drug Analysis. It has been accepted for inclusion in Journal of Food and Drug Analysis by an authorized editor of Journal of Food and Drug Analysis.

# Pomelo (*Citrus grandis* (L.) Osbeck) sponge layers as a potential source of soluble dietary fiber: Evaluation of its physicochemical, structural and functional properties

Xiaowei Chen<sup>a,1</sup>, Jiajia Chen<sup>a,1</sup>, Jian Peng<sup>a</sup>, Yuanshan Yu<sup>a</sup>, Jijun Wu<sup>a</sup>, Jing Wen<sup>a</sup>, Zhiying Kang<sup>b</sup>, Yanhui Wang<sup>b</sup>, Yujuan Xu<sup>a,\*\*</sup>, Lu Li<sup>a,\*</sup>

<sup>a</sup> Sericultural & Argi-Food Research Institute, Guangdong Academy of Agricultural Sciences/Key Laboratory of Functional Foods, Ministry of Agriculture and Rural Affairs/Guangdong Key Laboratory of Agricultural Products Processing, No.133 Yiheng Street, Dongguan Huang Road, Tianhe District, Guangzhou 510610, China

<sup>b</sup> Guangdong Xiangxue Wisdom Traditional Chinese Medicine Industry Co. Ltd., Guangzhou 510610, China

## Abstract

Pomelo sponge layer (PSL) had been considered as a potential source of soluble dietary fiber (SDF), while they were mostly disposed of as waste. To promote high-value utilization of pomelo wastes, this study extracted SDF from PSL of six varieties of pomelo, and their physicochemical, structural and functional properties were investigated. Results indicated that all PSL-SDFs showed good physicochemical and functional properties. Among them, PSL-SDF from grapefruit (GRSDF) showed better water holding capacity and swelling capacity, whereas Shatian pomelo PSL-SDF and Guanxi pomelo PSL-SDF had the highest thermal stability and oil holding capacity, respectively. Furthermore, compared with other PSL-SDFs, GRSDF displayed the lowest hydrolysis degree coupled with the best antioxidant and probiotic growth-promoting abilities. Finally, the correlation analysis showed that multiple beneficial effects of PSL-SDFs were markedly associated with their molecular weight and the concentrations of total phenolic, total flavonoids, rhamnose, galacturonic acid, glucose and arabinose. Collectively, these findings contributed to a better understanding of the physicochemical and functional properties of SDFs extracted from different PSLs, which provided a scientific basis for the development of PSL-SDFs into functional foods.

**Keywords:** Functional property, Physicochemical characteristics, Pomelo sponge layers, Soluble dietary fiber, Structure

## 1. Introduction

Dietary fiber (DF), defined as the edible fraction of plants or similar carbohydrates that were difficult to digest and absorb in the human small intestine, which was an important part of a healthy diet [1]. DF was mainly composed of cellulose, lignin, hemicellulose, gum, polysaccharides and oligosaccharides. According to its water solubility, DF could be divided into insoluble dietary fiber (IDF) and soluble dietary fiber (SDF). Although both SDF and IDF had multiple physiological activities, SDF presented better physiological functions [1].

Compared with IDF, SDF was more bioavailable as it could be degraded by ferulic acid esterase and glucosidases produced by some microorganisms in the intestine [2]. Moreover, SDF could be better utilized by gut bacteria, resulting in optimizing the host gut flora composition of the host [3]. Hence, SDFs had been considered as the emerging candidate prebiotics.

In the past, fibers such as wheat, corn and rice had been used for the production of SDF due to their health properties and technical features [4]. Nowadays, with the growing challenges of food security and environmental issues, there was an increased

Received 22 September 2023; accepted 30 November 2023.  
Available online 15 March 2024

\* Corresponding author.

\*\* Corresponding author.

E-mail addresses: xuyujuan@gdaas.cn (Y. Xu), lilu045@163.com (L. Li).

<sup>1</sup> Xiaowei Chen and Jiajia Chen contributed equally to this work.

<https://doi.org/10.38212/2224-6614.3489>

2224-6614/© 2024 Taiwan Food and Drug Administration. This is an open access article under the CC-BY-NC-ND license (<http://creativecommons.org/licenses/by-nc-nd/4.0/>).

interest in the high-value utilization of agricultural waste [5]. Additionally, consumer interested in healthy, nutritious and clean-labeled foods were on the rise. These trends had made the exploration of new sources of SDFs a hot topic in the research field. By-products of fruits and vegetables processing had been reported to be a rich source of novel and economical functional health ingredients, including peel, stems and cores [6]. However, these by-products were usually disposed of in the form of landfills or incineration, and small amounts were consumed through animal feed [5]. Therefore, it is necessary to develop some methods to utilize these by-products and wastes. Recently, several by-products such as orange pomace, tomato peel, and pineapple stems had been used as new sources of SDF [7].

Pomelo (*Citrus grandis* (L.) Osbeck) was a citrus fruit widely grown in China, Mexico and South Africa [8]. In addition to being eaten fresh, pomelo was often processed into juices, jams and other products to extend its shelf life [9]. During the processing of pomelo, a large amount of pomelo peel was produced, accounting for about 30–50% (w/w) of the fruit [10]. According to statistics, the annual global production of pomelo peel is about 2.8–4.7 million tons (FAO). In order to avoid environmental pollution and resource waste caused by a large number of by-products, it is particularly important to improve the utilization rate of pomelo peel [11]. Pomelo peel has been reported to contain epidermis and spongy layers, which was a potential source of high-quality DF [12]. Nowadays, there were growing studies on the pomelo sponge layer SDF (PSL-SDF), while they were mainly focused on the optimization of extraction methods, improvement of properties and application as a food additive [11–14]. In addition, varieties had a great influence on the physicochemical, structural and functional characteristics of SDF [15,16]. However, the differences in the physicochemical and functional properties of SDFs extracted from the sponge layer of different varieties of pomelo has not been elucidated. Meanwhile, fewer studies had been conducted on the gastrointestinal digestive tolerance of SDFs [11,14]. These issues hindered the development and application of PSL-SDF. Therefore, in order to better develop the PSL-SDF and in line with the concept of “green chemistry”, the sponge layers of several common Chinese varieties of pomelo were collected and a green extraction method (ultrasound combined with enzyme) was carried out to extract PSL-SDF. Subsequently, the physicochemical properties, structure, antioxidant activities, gastrointestinal tolerance and prebiotic activity of different PSL-SDFs were evaluated to establish a database of PSL-SDF.

## 2. Materials and methods

### 2.1. Materials

The sponge layers of pomelo peels used in this experiment were obtained from six ripe and fresh pomelo varieties (Grapefruit, Guanxi pomelo, Wendan pomelo, Liangping pomelo, Pingshan pomelo, and Shatian pomelo) that we collected from the main producing areas of pomelo in China. The detailed information on 6 varieties of pomelo were shown in Table S1. Six fruit trees of each variety and six fruits each tree was randomly collected for the experiment. After harvesting, all pomelo samples were immediately transported at 4 °C to Guangzhou. Chromatographic methanol (Cas. 67-56-1) and acetonitrile (Cas. 75-05-8) were supplied from Merck (Darmstadt, Germany). Gallic acid (Cas. 149-91-7), rutin (Cas. 153-18-4), mannose (Cas. 3458-28-4), ribose (Cas. 50-69-1), rhamnose (Cas. 6155-35-7), galacturonic acid (Cas. 91510-62-2), glucose (Cas. 50-99-7), galactose (Cas. 15572-79-9), xylose (Cas. 58-86-6), arabinose (Cas. 147-81-9) and fucose (Cas. 3615-37-0) purchased from Shanghai Yuanye Biotechnology Co., Ltd. (Shanghai, China). 2,2'-Azinobis (3-ethylbenzothiazoline-6-sulfonic Acid Ammonium Salt) (ABTS) (Cas. 30931-67-0), 1,1-Diphenyl-2-picrylhydrazyl radical 2,2-Diphenyl-1-(2,4,6-trinitrophenyl) hydrazyl (DPPH) (Cas. 1898-66-4), and potassium persulfate (Cas. 7727-21-1) were obtained from Shanghai Aladdin Biochemical Technology Co., Ltd. (Shanghai, China). Other analytically pure reagents: NaNO<sub>2</sub> (Cas. 7632-00-0), AlCl<sub>3</sub> (Cas. 7446-70-0), NaOH (Cas. 1310-73-2), NaCl (Cas. 7647-14-5), KCl (Cas. 7447-40-7), CaCl<sub>2</sub> (Cas. 10043-52-4), NaHCO<sub>3</sub> (Cas. 144-55-8), K<sub>3</sub>PO<sub>4</sub> (Cas. 7778-53-2), CH<sub>3</sub>COONa (Cas. 127-09-3), trifluoroacetic acid (Cas. 76-05-1) and trichloromethane (Cas. 67-66-3) were purchased from Tianjin Damao Chemical Reagent Factory (Tianjin, China). Water was purified by a Milli-Q system (Bedford, MA, USA).

### 2.2. Extraction of PSL-SDF from pomelos

The combined enzyme and ultrasound extraction method is an effective way to achieve higher yields of polysaccharide [17,18]. Therefore, the PSL-SDFs were extracted by enzyme and ultrasound synergistic method. The preparation process of PSL-SDFs from six variety pomelos was shown in Fig. 1. Pomelo fruitlets without visible external cuts or spoilage were selected, peeled, and washed. The pomelo sponge layer was collected and sliced with a knife to a thickness of <4 cm, followed by drying in an air blast oven at 55 °C for 24 h. The pomelo sponge layer was

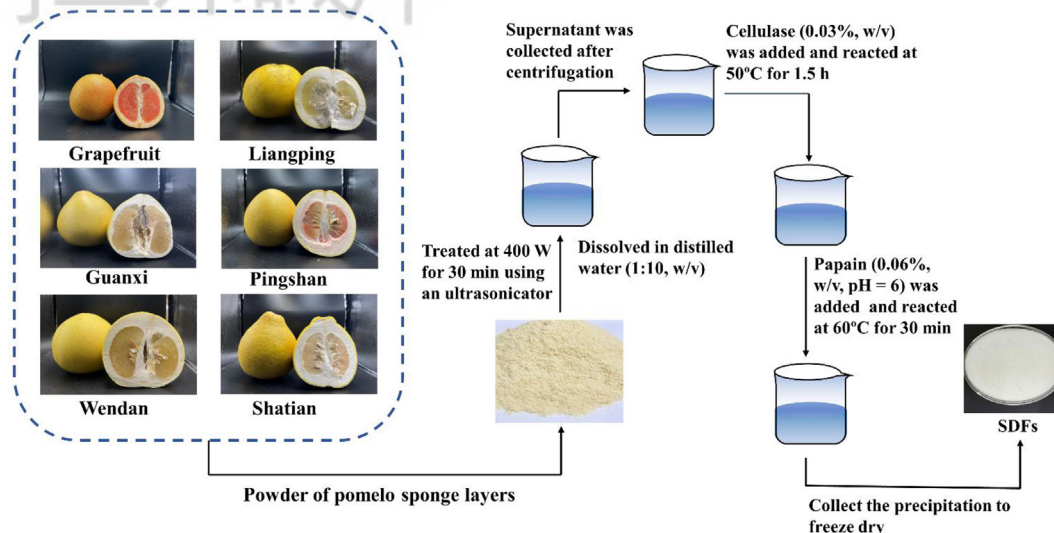


Fig. 1. Preparation process of PSL-SDFs. GRSDF, GUSDF, WESDF, LISDF, PISDF, and SHSDF presented the PSL-SDF extracted from Grapefruit, Guanxi pomelo, Wendan pomelo, Liangping pomelo, Pingshan pomelo, and Shatian pomelo, respectively.

ground to powder in a crusher and stored at  $-4^{\circ}\text{C}$  until use. The powder was mixed with distilled water (1:10, w/v) and treated at 400 W for 30 min using an ultrasonicator (DL-400B, Shanghai, China). After centrifugation at 5200 rpm for 15 min, the supernatant was collected and cellulase (0.03%, w/v, pH = 4.9) was added. The mixture was reacted at  $50^{\circ}\text{C}$  for 1.5 h. Subsequently, papain (0.06%, w/v, pH = 6) was added into the mixture and reacted at  $60^{\circ}\text{C}$  for 30 min. The reacted product was heated at  $90^{\circ}\text{C}$  for 10 min to inactivate the enzyme. The final mixture was concentrated and precipitated with 95% ethyl alcohol (1:4, v/v). The sediment was collected and freeze-dried to obtain PSL-SDFs. The lyophilized PSL-SDFs were milled using a grinder to pass through an 80-mesh sieve completely, except for those used for the determination of electron microscopy. The PSL-SDFs samples in powder form were stored in aluminum foil bags at  $-20^{\circ}\text{C}$  for further analysis. The PSL-SDFs extracted from the Grapefruit, Guanxi pomelo, Wendan pomelo, Liangping pomelo, Pingshan pomelo, and Shatian pomelo were abbreviated as GRSDF, GUSDF, WESDF, LISDF, PISDF and SHSDF, respectively.

### 2.3. Physicochemical properties of PSL-SDF

#### 2.3.1. Determination of ash, protein and fat

Ash, protein and fat contents were determined according to AOAC official method [19].

#### 2.3.2. Evaluation of water holding capacity (WHC), oil holding capacity (OHC) and swelling capacity (SC)

The sample ( $m_1$ , 0.5 g) was hydrated with 25 mL ultrapure water at room temperature for 2 h. After centrifugation at 4800 rpm for 10 min, the residue was immediately collected and weighed ( $m_2$ ). The WHC of sample was calculated using the following formula:

$$\text{WHC (g/g)} = (m_2 - m_1) / m_1$$

2.5 mL soybean oil was mixed with sample ( $m_1$ , 0.1 g) for 2 h at room temperature. After centrifugation at 4800 rpm for 10 min, the supernatant was removed and the precipitate was weighed ( $m_2$ ). The OHC of sample was computed by the following equation:

$$\text{OHC (g/g)} = (m_2 - m_1) / m_1$$

The sample ( $m$ , 0.05 g) was weighed and transferred to a 20 mL graduated test tube and mixed with 5 mL of distilled water. The mixture was stirred, defoamed, and left to stand for 18 h. The SC of sample was calculated by the following formula:

$$\text{SC (mL/g)} = (V_2 - V_1) / m$$

#### 2.3.3. Determination of total phenolics (TP) and total flavonoids (TF)

The concentration of TP was assessed by the Folin–Ciocalteu method [20]. The TP content of sample was presented as mg of gallic acid equivalents (GAE) per g of sample.



A 0.1 g of sample was added to 10 mL of 80% (v/v) methanol solution, ultrasonically extracted for 15 min, and centrifuged at 4000 rpm for 10 min. This procedure was repeated 2 times. 1 mL of supernatant was mixed with NaNO<sub>2</sub> (300 µL, 5%), AlCl<sub>3</sub> (300 µL, 10%) and 4 mL of 1 mol/L NaOH. Absorbance of the mixture was measured at 505 nm. The TF concentration was expressed as rutin equivalents (RE) mg/g.

#### 2.3.4. Molecular weight (Mw) analysis

The Mw of sample was determined by Advanced Polymer Chromatography (APC, Waters Corp., Milford, MA, USA). 4 mg sample was dissolved in 2 mL of ultrapure water, then the mixture was filtered through a 0.45 µm aqueous membrane. The column temperature was 25 °C and ultrapure water was the mobile phase at a flow rate of 1.0 mL/min. Data were collected and analyzed using Empower software.

#### 2.3.5. Thermal analysis

The thermal properties of the sample were detected by a differential scanning calorimetry (DSC200F3, NETZSCH, Germany). A 6 mg sample was first weighed for later determination, and the crucible without sample acted as the reference. Nitrogen gas (N<sub>2</sub>) was injected into the machine at 0.06 mPa, and the sample was heated from 30 °C to 300 °C with a linear ramping of 10 K/min. Data were recorded and analyzed using the Netzsch software (Netzsch Inc., Selb, Germany).

### 2.4. Structural characteristics of PSL-SDF

#### 2.4.1. Scanning electron microscopy (SEM) analysis

The morphology and microstructure of sample were analyzed by a SEM (S-3700N, Hitachi, Japan). Sample was placed on double-sided tape and coated with a thin layer of gold. Images were collected at an accelerating voltage of 3.0 kV. Micrographs were recorded at 100 × magnification.

#### 2.4.2. Fourier-transform infrared spectroscopy (FT-IR) analysis

The functional groups of samples were measured by a FT-IR (Nicolet IS50, Bruker, Germany) in the range of 400–4000 cm<sup>-1</sup>. Each 5 mg sample was mixed with 100 mg KBr, and the mixture was ground and pressed into tablets. These scans were compared with a blank KBr background.

#### 2.4.3. X-ray diffraction (XRD) analysis

XRD analysis of sample was performed with an X-ray diffractometer (D8 ADVANCE, Bruker, Germany). The incident current and copper radiation

were 40 mA and 40 kV, respectively. The scanning speed was 12°/min and the step length was 0.013°, the diffraction angle (2θ) ranged from 5° to 60°. The degree of crystallinity (DC, %) was calculated using the following equation:

$$DC(\%) = \frac{A_c \times 100}{(A_c + A_a)}$$

where A<sub>c</sub> and A<sub>a</sub> denoted the crystalline and amorphous regions on the X-ray diffraction map, respectively.

#### 2.4.4. Monosaccharide composition analysis

The monosaccharide composition of sample was analyzed by high performance liquid chromatography (HPLC, LC-20AT; Shimadzu Co., Ltd., Tokyo, Japan) with an Agilent packed column (ZORBAXE eclipse XDB-C18, 4.6 mm × 250 mm). 0.01 g of SDF was mixed with 2 mL of 2 mol/L trifluoroacetic acid, and the mixture was hydrolyzed at 100 °C for 8 h. Then the hydrolysate was mixed with 0.5 mol/L 1-phenyl-3-methyl-5-pyrazolone solution and reacted at 70 °C for 1 h. After neutralization, the solution was extracted three times with 3 mL chloroform. Then, mannose (Man), ribose (Rib), rhamnose (Rha), galacturonic acid (Gala), glucose (Glu), galactose (Gal), xylose (Xyl), arabinose (Ara) and fucose (Fuc) mixed monosaccharide solutions (concentration gradient including 0.6, 1.2, 2.4, 3.6, 4.8 and 6 mg/mL) were prepared. All solutions were filtrated through 0.22 µm for testing. Chromatographic separation was carried out using 0.05 M potassium phosphate buffer (pH 6.85) and acetonitrile at a ratio of 85:15 (v:v) as mobile phase. The flow rate was 1 mL/min.

### 2.5. Functional properties of PSL-SDF

#### 2.5.1. Antioxidant capacity analysis

1 mL sample solution (5 mg/mL) was mixed with 5 mL 130 µmol/L DPPH. The mixture was reacted in the dark for 30 min and then centrifuged at 4800 rpm/min for 10 min. The supernatant was removed and absorbance values were measured at 517 nm. The 1 mL distilled water mixed with 5 mL 130 µmol/L DPPH was used as a blank control. The DPPH radical scavenging ability was computed based on the following equations:

$$DPPH \text{ radical scavenging ability } (\%) = (A_0 - A_1) \times 100 / A_0$$

where A<sub>0</sub> = absorbance value of blank control; A<sub>1</sub> = absorbance value of sample.

50 mL of 7 mmol/L ABTS solution was mixed with 0.88 mL of 140 mmol/L potassium persulfate and allowed to stand in the dark for 14 h. The mixture

was diluted with methanol (80%, v/v) to an absorbance of 0.70. 100  $\mu$ L of 5 mg/mL sample solution was then added to 3.6 mL diluted solution and the mixture was reacted in the dark for 30 min. The absorbance of mixture was measured at 734 nm. The ABTS radical scavenging capacity was calculated using the formula below:

$$\text{ABTS radical scavenging capacity (\%)} \\ = (A_0 - A_1) \times 100 / A_0$$

where  $A_0$  presented the absorbance value of blank control, and  $A_1$  indicated the absorbance value of sample.

#### 2.5.2. Simulated gastric and intestinal digestion in vitro

*In vitro* simulated gastric fluid digestion: 500 mL of gastric electrolyte solution (3.1 g/L NaCl, 1.2 g/L KCl, 0.2 g/L  $\text{CaCl}_2$  and 0.7 g/L  $\text{NaHCO}_3$ ) was mixed with pepsin (0.12 g), lipase (0.13 g) and  $\text{CH}_3\text{COONa}$  solution (1 mol/L, 10 mL). The final pH of mixture was adjusted to 2 by addition of 0.1 mol/L HCl, resulting in simulated gastric juice. Sample (2 mg/mL) was dissolved in 10 mL of simulated gastric juice as the experimental group. The control group was an equal volume of simulated gastric juice. Both experimental group and control group were reacted in a dioxide-water system at 37 °C for 6 h. Samples were analyzed after 0, 2, 4 and 6 h of digestion.

*In vitro* simulated small intestinal digestion: 100 g of small intestinal salt solution (5.4 g/L NaCl, 0.7 g/L KCl, 0.4 g/L  $\text{CaCl}_2$ , 1 mol/L  $\text{NaHCO}_3$ , pH = 7) was added to 13 mg trypsin, 400 mL of bile salt solution (4%, w/w) and 100 g of trypsin solution (7%, w/w). The pH of the simulated small intestine solution was adjusted to 7.5 with 0.1 mol/L NaOH solution. 3 mL of simulated small intestine solution was mixed with 10 mL of simulated gastric juice, which was set as group A. 3 mL of distilled water mixed with 10 mL of simulated gastric juice was set as group B, and the 3 mL of simulated small intestine solution mixed with 10 mL of distilled water was set as group C. Each group was reacted in a dioxide-water system at 37 °C for 6 h. Samples were analyzed after 0, 2, 4 and 6 h of digestion.

To determine whether sample was degraded in gastric juice and small intestinal solution, the total sugars (TS) content, reducing sugars (RS) content and the degree of hydrolysis were measured after digestion. TS content was determined by the phenol-sulphate method. The degree of hydrolysis was computed by the following formula:

$$\text{Hydrolysis degree (\%)} = C_1 / (C_2 - C_3) \times 100\%$$

where  $C_1$  was the content of hydrolyzed RS,  $C_2$  was the content of TS, and  $C_3$  was the content of initial RS (0 h).

#### 2.5.3. Probiotics growth

Using a modified carbohydrate-free medium to evaluate the effects of PSL-SDF on the growth of probiotics. Four probiotics (*Leuconostoc mesenteroides*, *Lactobacillus acidophilus*, *Lactobacillus casei* and *Bifidobacterium*) were used in this experiment. Modified carbohydrate-free medium was composed of 0.2 g/L peptone, 0.2 g/L yeast extract, 5 g/L  $\text{CH}_3\text{COONa}$ , 2 g/L triammonium citrate, 1.08 g/L Tween 80, 0.3 g/L  $\text{MgSO}_4 \cdot 7\text{H}_2\text{O}$ , 0.07 g/L  $\text{MnSO}_4 \cdot \text{H}_2\text{O}$ , 1.53 g/L  $\text{K}_2\text{HPO}_4$ . The modified carbohydrate-free medium supplemented with SDF (5 mg/mL), inulin (5 mg/mL) and glucose (5 mg/mL) were set as experimental group, positive control group 1 and positive control group 2, respectively. These four probiotics were inoculated into MRS broth and incubated at 37 °C for 24 h to prepare seed culture. Seed culture (inoculum size 3%) was transferred into the corresponding medium. The growth of probiotic was assessed by measuring the bacterial populations of the medium after incubation for 0 h, 12 h, and 24 h. Bacterial populations was performed by plate counting method, and the bacteria count was expressed as colony forming units per milliliter (CFU/mL). A pH meter was used to detect the pH of medium at 0 h, 12 h, and 24 h of bacterial fermentation.

#### 2.6. Statistical analysis

All measurements were performed at least in triplicate, and the data were expressed as mean  $\pm$  standard deviation (SD). Significant differences between means were determined by Duncan's multiple range test in SPSS software version 26.0 (IBM Corporation, Armonk, NY, USA).  $P < 0.05$  was considered to reflect a statistically significant difference.

### 3. Results and discussion

#### 3.1. Ash, fat, protein and Mw of different PSL-SDFs

Firstly, the proximate composition of PSL-SDFs from different pomelos was measured. As shown in Table 1, the ash, protein and fat contents of different PSL-SDFs were ranged of 1.49–4.30 wt%, 0.23–0.41 wt%, and 0.02–0.25 wt%, respectively. The fat contents of GRSDF, GUSDF, WESDF, and LISDF were all between 0.02 and 0.7 wt%. The ash

Table 1. The physicochemical properties and monosaccharide composition of different PSL-SDFs.

	GRSDF	GUSDF	WESDF	LISDF	PISDF	SHSDF
Ash (wt%)	1.49 ± 0.05 <sup>f</sup>	4.30 ± 0.00 <sup>a</sup>	2.92 ± 0.02 <sup>d</sup>	3.96 ± 0.05 <sup>b</sup>	2.15 ± 0.01 <sup>e</sup>	3.25 ± 0.03 <sup>c</sup>
Fat (wt%)	0.07 ± 0.00 <sup>c</sup>	0.03 ± 0.00 <sup>c</sup>	0.02 ± 0.00 <sup>c</sup>	0.02 ± 0.00 <sup>c</sup>	0.25 ± 0.02 <sup>b</sup>	0.33 ± 0.01 <sup>a</sup>
Protein (wt%)	0.37 ± 0.03 <sup>b</sup>	0.41 ± 0.02 <sup>a</sup>	0.38 ± 0.02 <sup>ab</sup>	0.23 ± 0.01 <sup>e</sup>	0.29 ± 0.00 <sup>d</sup>	0.33 ± 0.02 <sup>c</sup>
WHC (g/g)	19.52 ± 0.68 <sup>a</sup>	18.83 ± 0.70 <sup>a</sup>	13.57 ± 0.11 <sup>bc</sup>	13.81 ± 0.30 <sup>b</sup>	12.68 ± 0.68 <sup>c</sup>	14.65 ± 0.71 <sup>b</sup>
OHC (g/g)	7.59 ± 0.18 <sup>c</sup>	11.05 ± 0.21 <sup>a</sup>	8.89 ± 0.54 <sup>b</sup>	3.32 ± 0.05 <sup>e</sup>	5.21 ± 0.03 <sup>d</sup>	7.28 ± 0.48 <sup>c</sup>
SC (mL/g)	55.41 ± 4.94 <sup>a</sup>	47.51 ± 3.12 <sup>b</sup>	41.89 ± 2.04 <sup>bc</sup>	25.93 ± 1.92 <sup>d</sup>	37.78 ± 2.91 <sup>c</sup>	46.48 ± 3.07 <sup>b</sup>
Mw (kDa)	124.81 ± 0.65 <sup>f</sup>	218.95 ± 0.59 <sup>d</sup>	237.19 ± 0.56 <sup>c</sup>	273.24 ± 0.60 <sup>b</sup>	200.36 ± 0.48 <sup>e</sup>	302.28 ± 0.24 <sup>a</sup>
TP (mg RE/g)	31.45 ± 1.01 <sup>a</sup>	13.88 ± 0.54 <sup>bc</sup>	14.69 ± 0.80 <sup>b</sup>	11.96 ± 0.56 <sup>d</sup>	13.41 ± 0.36 <sup>c</sup>	9.06 ± 0.33 <sup>e</sup>
TF (mg GAE/g)	3.82 ± 0.02 <sup>a</sup>	2.34 ± 0.04 <sup>c</sup>	2.98 ± 0.02 <sup>b</sup>	1.65 ± 0.07 <sup>d</sup>	2.97 ± 0.06 <sup>b</sup>	1.47 ± 0.04 <sup>e</sup>
Man (mg/g)	2.07 ± 0.06 <sup>ab</sup>	2.20 ± 0.16 <sup>ab</sup>	1.65 ± 0.35 <sup>c</sup>	2.43 ± 0.27 <sup>a</sup>	2.02 ± 0.16 <sup>b</sup>	1.03 ± 0.04 <sup>d</sup>
Rib (mg/g)	ND	3.17 ± 0.40 <sup>c</sup>	3.87 ± 0.34 <sup>b</sup>	2.12 ± 0.07 <sup>d</sup>	4.58 ± 0.05 <sup>a</sup>	3.89 ± 0.16 <sup>b</sup>
Rha (mg/g)	7.17 ± 0.38 <sup>a</sup>	0.39 ± 0.08 <sup>d</sup>	0.35 ± 0.04 <sup>d</sup>	1.40 ± 0.12 <sup>c</sup>	2.15 ± 0.34 <sup>b</sup>	ND
Gala (mg/g)	1.90 ± 0.06 <sup>b</sup>	2.14 ± 0.36 <sup>ab</sup>	2.60 ± 0.25 <sup>a</sup>	ND	ND	ND
Glu (mg/g)	222.70 ± 3.29 <sup>a</sup>	122.98 ± 1.84 <sup>c</sup>	131.52 ± 2.19 <sup>c</sup>	48.91 ± 1.55 <sup>d</sup>	63.18 ± 0.36 <sup>d</sup>	153.88 ± 2.02 <sup>b</sup>
Gal (mg/g)	13.31 ± 0.24 <sup>b</sup>	ND	ND	18.67 ± 0.45 <sup>a</sup>	9.86 ± 0.33 <sup>c</sup>	ND
Xyl (mg/g)	3.62 ± 0.20 <sup>c</sup>	3.57 ± 0.37 <sup>c</sup>	4.14 ± 0.30 <sup>b</sup>	2.44 ± 0.20 <sup>d</sup>	1.90 ± 0.19 <sup>d</sup>	6.90 ± 0.54 <sup>a</sup>
Ara (mg/g)	16.19 ± 0.04 <sup>a</sup>	6.04 ± 0.13 <sup>d</sup>	5.86 ± 0.63 <sup>d</sup>	6.69 ± 0.24 <sup>c</sup>	10.13 ± 0.84 <sup>b</sup>	3.55 ± 0.20 <sup>e</sup>
Fuc (mg/g)	ND	ND	ND	ND	ND	ND

Results were expressed as means ± standard deviation (n = 3). n = 3 means that the repeated experiments were carried out three times. Values with different letters in each row were significantly different ( $P < 0.05$ ). GRSDF, GUSDF, WESDF, LISDF, PISDF, and SHSDF presented the PSL-SDF extracted from Grapefruit, Guanxi pomelo, Wendan pomelo, Liangping pomelo, Pingshan pomelo, and Shatian pomelo, respectively.

concentrations of PSL-SDFs ranged from 1.49 to 4.30 wt%, which were lower than that of Belgian endive (*Cichorium intybus* var. *foliosum*) by-products fibers [4]. Among these six PSL-SDF samples, GUSDF presented the highest contents of ash (43.01 g/kg) and protein (4.1 g/kg). The lowest ash content of 14.93 g/kg was observed in GRSDF, which was consistent with a previous study [12]. Moreover, the protein contents of all PSL-SDFs were less than 64.6 g/kg, which were comparable to commercial citrus fiber [13]. In addition, the Mw of different PSL-SDFs was also analyzed. Significant differences were existed in the Mw of different PSL-SDF samples (Table 1). Among these six PSL-SDFs, SHSDF exhibited the highest Mw (302.28 kDa), followed by PISDF (273.24 kDa), WESDF (237.19 kDa), and GUSDF (218.95 kDa). Above results suggested that the proximate composition and Mw of PSL-SDF from different variety pomelos differed significantly.

### 3.2. WHC, OHC and SC of different PSL-SDFs

To further evaluate the physicochemical properties of SDFs extracted from pomelo sponge layers, the WHC, OHC and SC of PSL-SDFs were analyzed. It is well known that WHC and SC are two hydration properties of SDF that are important in the ability of SDF to promote human defecation [21]. As indicated in Table 1, the WHC and SC of different PSL-SDFs had great variation. According to previous research, the WHC and SC of commercial citrus SDF were 11.90 g/g and 16.44 mL/g, respectively, which were

both lower than those of these six PSL-SDFs [22]. Among the six PSL-SDFs, GRSDF showed higher WHC (19.52 g/g) and SC (55.41 mL/g) in comparison with other PSL-SDF samples, indicating that GRSDF might have a better capacity of promoting human defecation. As is well known, OHC could reflect the ability of SDF to absorb fat [12]. The highest OHC was found in GUSDF (11.05 g/g), while LISDF obtained the lowest OHC (3.32 g/g). Hence, it could be presumed that GUSDF might have a better capacity of promoting fat excretion than LISDF. Furthermore, the OHC of SDF often had a close relationship with its protein content [23], and this result was also observed in these six PSL-SDFs. Above results indicated that PSL-SDFs had the potential to be used in the food industry.

### 3.3. Thermal stability of different PSL-SDFs

DSC is a thermodynamic technique used to determine the thermal properties and stability of macromolecules [16]. Therefore, DSC analysis was used to evaluate the thermal stability of PSL-SDF samples. As shown in Fig. 2A, all PSL-SDFs showed a 2-step thermal decomposition. Significant variations in these samples occurred mainly in the temperature range of 10–150 °C and 200–250 °C. The first endothermic peak of PSL-SDFs transited in the range of 50–120 °C. The onset and end temperatures of the first peak (water release) were ranged from 19.13 to 59.37 °C and 77.06–150.00 °C, respectively (Table S2). It was probably due to the transformation

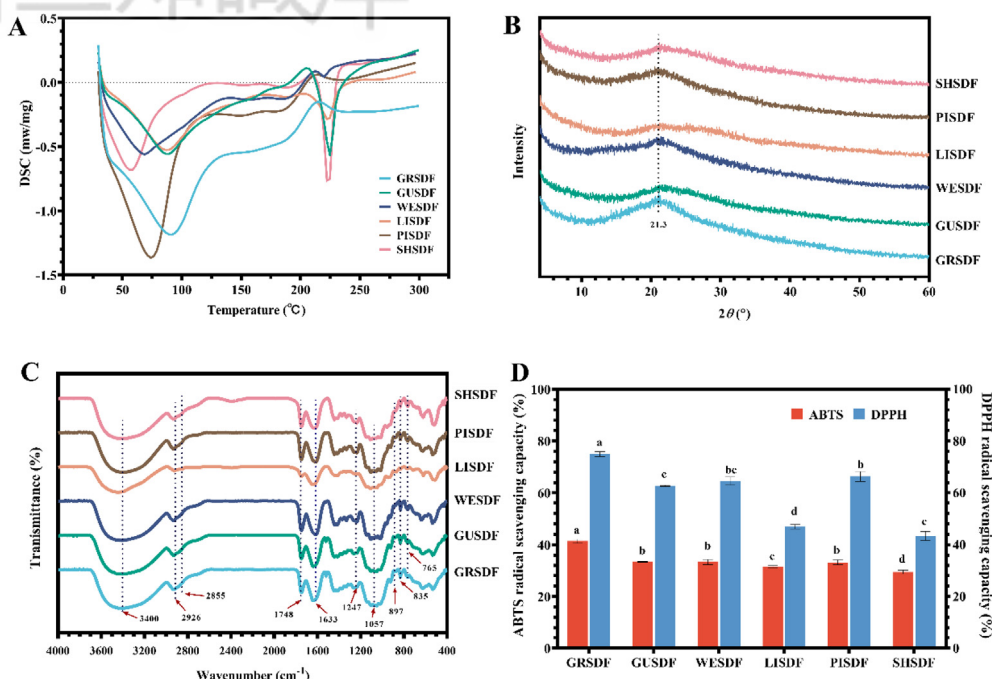


Fig. 2. Thermal stability (A), FT-IR spectroscopy (B), XRD patterns (C) and antioxidant activities (D) of different PSL-SDFs. GRSDf, GUSDF, WESDF, LISDF, PISDF, and SHSDF presented the PSL-SDF extracted from Grapefruit, Guanxi pomelo, Wendan pomelo, Liangping pomelo, Pingshan pomelo, and Shatian pomelo, respectively.

of water adsorbed by SDF from a crystalline to the amorphous structure and the evaporation of free water [24]. The maximum enthalpy change ( $\Delta H$ ) of the first phase peak was found in PISDF ( $-270.5$  J/g), indicating that PISDF might contain more free water and crystal-bound water. In general, the magnitude of the exothermic enthalpy change was negatively correlated with the thermal stability. Substances that required higher temperatures for decomposition were generally considered to be more thermally stable [25]. GRSDf and PISDF showed exothermic peaks in the second stage with exothermic enthalpy changes of  $24.41$  J/g and  $22.21$  J/g, respectively. Increased temperature led to the decomposition of cellulose and hemicellulose, resulting in the gradual depolymerization of macromolecules and the appearance of exothermic peak [26]. Above results demonstrated that the PISDF and GRSDf had lower thermal stabilities than other four PSL-SDFs.

### 3.4. Functional groups of different PSL-SDFs

FT-IR spectroscopy could reflect the functional groups of polysaccharides and the bonding relationships between them. Hence, FT-IR spectroscopy was used to further analyze the structure of PSL-SDFs. The FT-IR spectra of all samples exhibited similar characteristics (Fig. 2B). Specifically, strong absorption peaks at around  $3400$   $\text{cm}^{-1}$  with a

broad peak shape were observed, which was ascribed to  $-\text{OH}$  stretching vibration. The absorption bands at  $2926$   $\text{cm}^{-1}$  and  $2855$   $\text{cm}^{-1}$  corresponded to the typical absorbance of polysaccharide-based polymers the C-H vibration of the polysaccharide methylene, which was the typical of the polysaccharide structure [27]. The peak in the  $1200$ – $1800$   $\text{cm}^{-1}$  wavelength range was related to the C-O-C and C-O-H vibrations of the sugar ring [28]. The strong main peak at  $1633$   $\text{cm}^{-1}$  was caused by the  $-\text{C}=\text{O}$  and valence vibrations in the carboxyl group, which could be considered as a binding site for calcium ions, indicating that all PSL-SDFs could form stronger gels [29]. The absorption peak at  $1748$   $\text{cm}^{-1}$  was the  $-\text{CO}$  stretch of  $-\text{COOH}$ . The low intensity peak at  $897$   $\text{cm}^{-1}$  indicated the presence of mannose bonds [25]. The peaks at  $835$   $\text{cm}^{-1}$  and  $735$   $\text{cm}^{-1}$  represented the  $\alpha$ -glycosidic bond stretching vibration and the D-glucopyranose ring structure in polysaccharides, respectively.

### 3.5. Crystalline property of different PSL-SDFs

XRD is a powerful technique used for revealing the crystalline structure of polymers [16]. The structural property of PSL-SDFs was also evaluated by XRD analysis, and the result was presented in Fig. 2C. All PSL-SDF samples exhibited coexistence of crystalline and non-crystalline states. The same



diffraction peak ( $2\theta = 21^\circ$ ) was observed in all PSL-SDF samples, which was in agreement with previous studies [30]. This result indicated that all the samples had the recognized crystalline structure of SDF. Therefore, the relative crystallinity of the all PSL-SDF samples were calculated. Generally, the smaller the molecular weight of a substance, the higher the degree of crystallinity [31]. The highest relative crystallinity (26.52%) was found in GRSDf, followed by PISDF (23.54%), which was in agreement with Mw results (Table 1). The Mw was reported to be strongly affected by raw material [32]. Accordingly, the difference in relative crystallinity of these six PSL-SDFs might be due to the difference in raw material.

### 3.6. Microstructure of different PSL-SDFs

SEM images exhibited that all PSL-SDF samples had lamellar structures, except for LISDF, which had a large number of holes on its surface (Fig. 3). Meanwhile, some small clusters and spherical substances were also found on the surface of LISDF. The LISDF exhibited a compact texture with a wrinkled surface, cracks and holes, most likely as a result of residual proteins [33]. According to a previous study, the microstructure of GRSDf extracted by heated water method was dense and disorganized with many irregular filaments [12], which was different from the result of this study. This difference might be attributed to the different extraction method. In this study, the extraction of PSL-SDF using ultrasound combined with enzyme method, which could enlarge the pores of the plant material

cell walls, resulting a large number of pores on the surface of SDF [34]. The surface of SDF with more pores could improve its WHC, OHC and SC [35]. Hence, the GRSDf extracted by ultrasound combined with enzyme method had higher WHC, OHC and SC than the GRSDf extracted by heated water method [12].

### 3.7. Monosaccharide composition of different PSL-SDFs

Table 1 showed the monosaccharide composition of different PSL-SDFs, in which eight monosaccharides (Man, Rib, Rha, Gala, Glu, Gal, Xyl and Ara) were detected. However, the Fuc was not detected in any of the PSL-SDF samples, which was possible that ultrasound disrupted the glycosidic bonds of Fuc in the PSL-SDF samples [35]. Among these detected monosaccharides, Man, Glu, Xyl and Ara were detected in all PSL-SDFs. The Glu (59.21–87.70%) was the most abundant monosaccharide in all PSL-SDFs, suggesting that all PSL-SDF samples were mainly made of  $\beta$ -glucan based substrates [36]. The Ara was another main monosaccharide in PSL-SDFs, which was similar to that in SDFs extracted from orange peel [37]. In contrast, the Man and Xyl contents were at low levels in all PSL-SDF samples. For the other four monosaccharides (Rib, Rha, Gala, and Gal), they were detected in different PSL-SDF samples. Among them, the Rib was detected in all PSL-SDFs except GRSDf, while the Rha was detected in all PSL-SDFs except SHSDF. Meanwhile, the Gal was only detected in GRSDf, LISDF and PISDF, whereas the

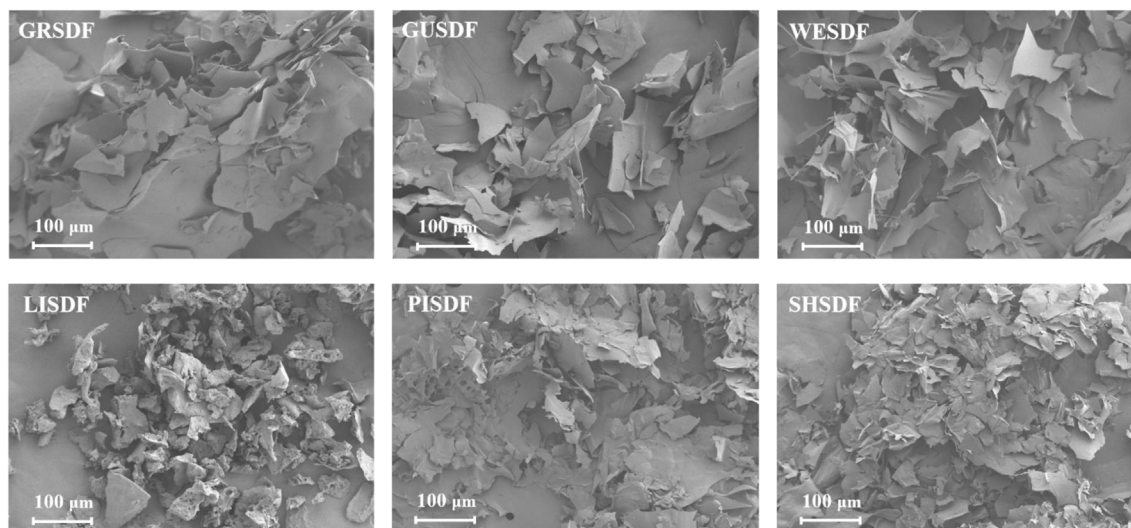


Fig. 3. SEM images of different PSL-SDFs. GRSDf, GUSDF, WESDF, LISDF, PISDF, and SHSDF presented the PSL-SDF extracted from Grapefruit, Guanxi pomelo, Wendan pomelo, Liangping pomelo, Pingshan pomelo, and Shatian pomelo, respectively.

Gala was only detected in GRSDf, GUSDF and WESDF. The above results indicated that there were differences in the monosaccharide composition of different PSL-SDF samples, which might have an impact on their structural characterization and functional activity [15].

### 3.8. Bioactive compounds and antioxidant activity of different PSL-SDFs

Pomelo fruitlets were rich in phenolics and flavonoids, which had the capacities of antioxidant activities and reducing the risk of inflammation, mutagenesis and carcinogenesis [38]. Many scholars had found that the TP, TF and antioxidant activities of SDF were great influenced by its raw materials [39]. Therefore, the levels of TP, TF (Table 1) and antioxidant activity (Fig. 2D) of PSL-SDFs were analyzed. GRSDf had the highest TP (31.45 mg RE/g) and TF (3.82 mg GAE/g) contents, while the lowest TP (9.06 mg RE/g) and TF (1.47 mg GAE/g) concentrations were found in SHSDF. Compared with other PSL-SDF samples, the GRSDf showed the highest antioxidant activity. At the same time, the lowest antioxidant capacity was observed in SHSDF. Above results suggested that the TP and TF contents of PSL-SDFs had a positive relationship with its antioxidant activity. Moreover, previous studies had shown that the antioxidant ability of SDF also had a correlation with its Mw, and the higher the Mw of SDF, the lower its antioxidant capacity [40]. Among these PSL-SDFs, GRSDf exhibited the lowest Mw coupled with the highest antioxidant ability.

### 3.9. Digestion tolerance of different PSL-SDFs

The analysis of the tolerance of polysaccharides to gastrointestinal digestion could be used to determine whether they could be applied as prebiotics to regulate the composition and metabolism of host gut microbes [41]. Therefore, the resistance of PSL-SDFs to gastrointestinal digestion was analyzed (Fig. 4). The hydrolysis degree of PSL-SDF was used to evaluate its tolerance, and the higher hydrolysis degree of PSL-SDF, the poorer its resistance to gastrointestinal digestion. As shown in Fig. 4A, both the PSL-SDF group and control group showed a great increase in hydrolysis degree after 2 h of digestion in simulated gastric juice. When food was retained in the human stomach, the gastric juices were usually released within 2 h [42]. Therefore, the rate of increase in hydrolysis was higher from 0 to 2 h than in other digestive time periods. Moreover, the TS content of all PSL-SDF

groups decreased with increasing digestion time, while the reduce in TS content of GRSDf group after 6 h digestion in simulated gastric fluid was lower than that of other PSL-SDFs. Meanwhile, the lowest increase rate (7.35%) of RS content was observed in GRSDf group after *in vitro* simulated gastric digestion, which was much lower than that in the other PSL-SDFs. Hence, after *in vitro* simulated gastric digestion, a lower hydrolysis degree of PSL-SDF was found in GRSDf in comparison with other PSL-SDFs. A previous study also reported that during the digestion of *Plantago asiatica* L. seed SDF by gastric juice, the TS content in the digestate decreased with increasing digestion time, while RS content increased [43]. In the *in vitro* simulated digestion phase, the conversion of TS to RS was due to the enzymatic disruption of the PSL-SDF glycosidic bond and the formation of reducing ends [44].

Nevertheless, during simulated intestinal fluid digestion, no significant changes in TS and RS contents were found in both experimental and control groups at different digestion times (Figs. 4B, 5C and 5D). Moreover, there was essentially no increase in the hydrolysis of all PSL-SDF groups compared to the blank control group B, suggesting that all the PSL-SDFs had strong anti-digestive properties in the intestine. All PSL-SDFs were digested to varying degrees as they passed through simulated gastrointestinal liquid, while at least 50% of the PSL-SDF would reach the colon. After simulated gastrointestinal digestion, PISDF obtained the highest hydrolysis level (43.73%), while the lowest hydrolysis level (17.19%) was found in GRSDf, revealing that GRSDf had the best digestive resistance in comparison with other SDFs.

### 3.10. Promotion probiotics growth capacity of different PSL-SDFs

Based on previous researches, SDF was usually considered to have the ability to promote the growth of probiotics [45]. Hence, the promotion probiotics growth capacity of PSL-SDFs was evaluated. No significant change in probiotics numbers and pH values was found in the blank control group during fermentation (Fig. 4A, B, C, and D), indicating that the modified carbohydrate-free medium employed in the present study was a reliable choice for prebiotic activity experiments. Compared with the blank control group, PSL-SDF and positive control groups presented more probiotics populations coupled with lower pH values. This result suggested that all the PSL-SDFs could promote the growth of *L. mesenteroides*, *L. acidophilus*, *L. casei*

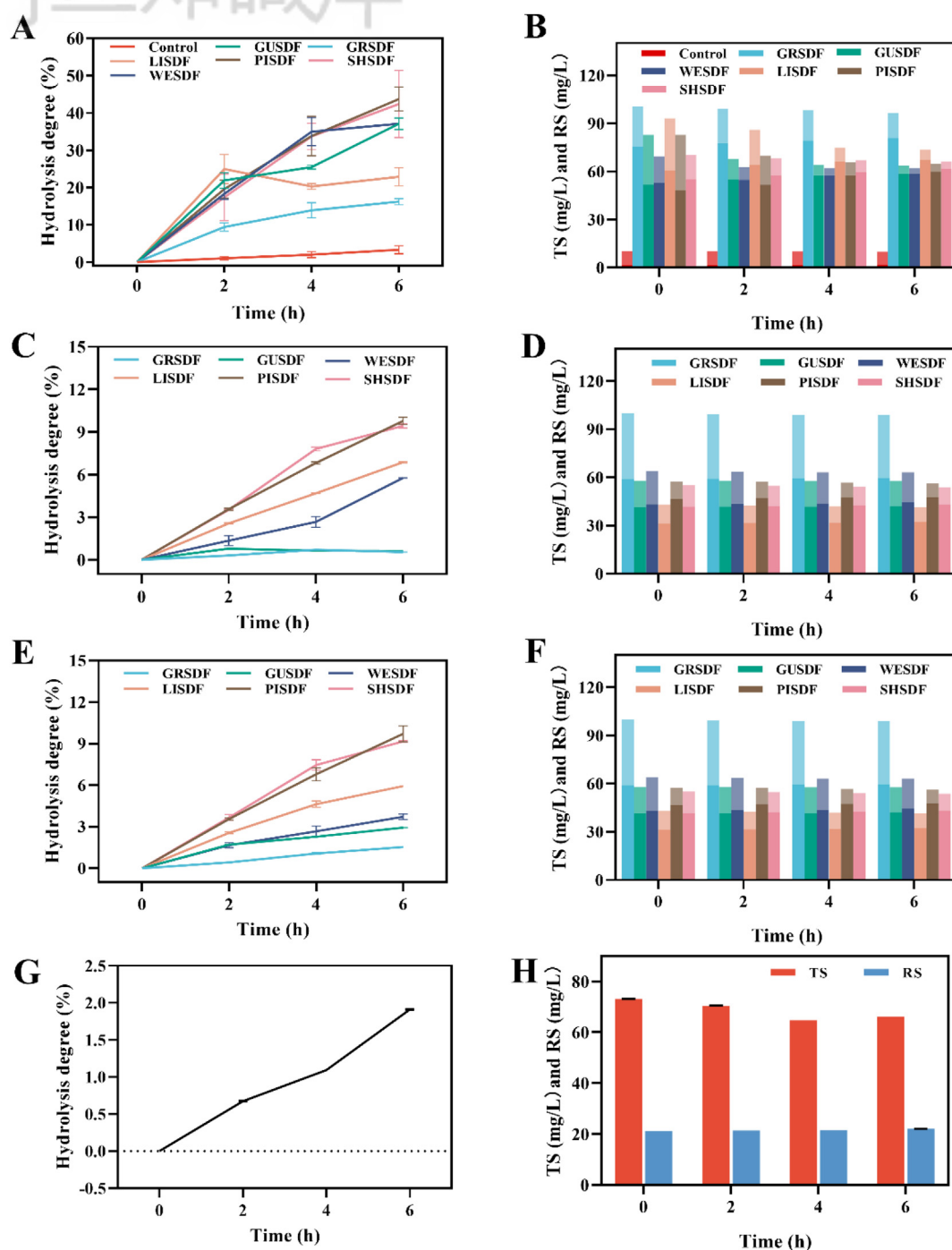


Fig. 4. Digestion tolerance of different PSL-SDFs. (A) Gastric fluid simulation; (B) Experimental group A for intestinal fluid simulation; (C) Control group B for intestinal fluid simulation; (D) Control group C for intestinal fluid simulation. Lighter bars of the same color in the graph indicate TS content and darker bars indicate RS content. GRSDf, GUSDF, WESDF, LISDF, PISDF, and SHSDF presented the PSL-SDF extracted from Grapefruit, Guanxi pomelo, Wendan pomelo, Liangping pomelo, Pingshan pomelo, and Shatian pomelo, respectively.

and *Bifidobacterium*, which might be due to their monosaccharide composition. The glucose was the main monosaccharide of PSL-SDFs, which was widely existed in the prebiotic [46]. After cultured for 48 h, the populations of the four probiotics in MRS medium supplemented with GRSDf were

significantly higher than those in medium supplemented with other PSL-SDFs. Moreover, PISDF also exhibited a higher promotion probiotics growth capacity than GUSDF, LISDF, and SHSDF. These results could be attributed to the GRSDf and PISDF had a lower Mw. The Mw of polysaccharides

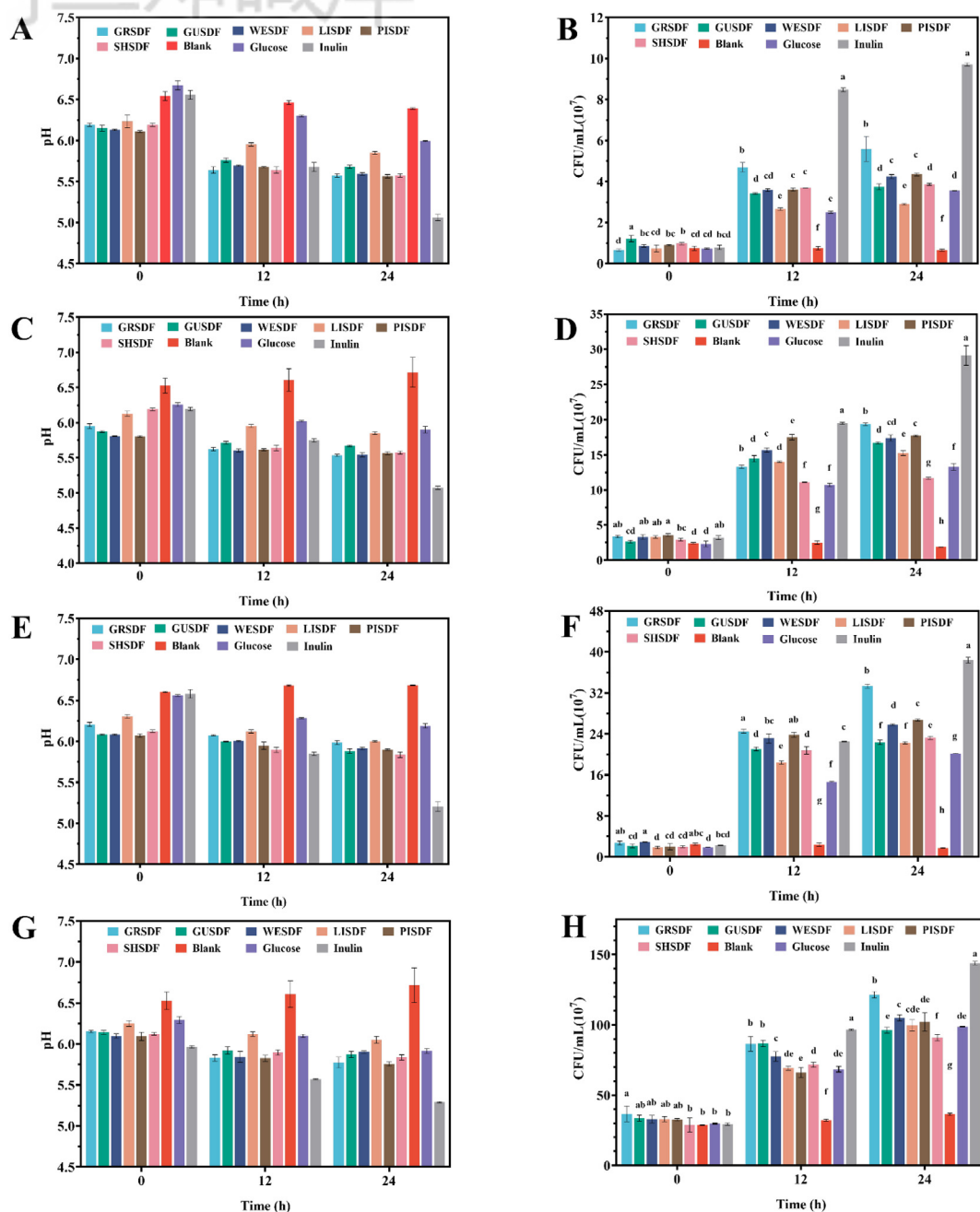


Fig. 5. Effect of different PSL-SDFs on the growth of *Leuconostoc mesenteroides* (A), *Lactobacillus acidophilus* (B), *Lactobacillus casei* (C), and *Bifidobacterium* (D). GRSDF, GUSDF, WESDF, LISDF, PISDF, and SHSDF presented the PSL-SDF extracted from Grapefruit, Guanxi pomelo, Wendan pomelo, Liangping pomelo, Pingshan pomelo, and Shatian pomelo, respectively.

had a great impact on their utilization by probiotics, the lower the Mw of polysaccharides, the easier they could be utilized by probiotics [47].

### 3.11. Correlation among the raw materials, structural property, bioactive compounds and functional characteristic of PSL-SDFs

To disclose the relationship of raw materials, structure, bioactive compounds and activity

functional characteristic of different PSL-SDFs, spearman correlation analysis and principal component analysis (PCA) were performed (Fig. 6A, B and C). As presented in Fig. 6A, Mw, TP, TF, Rib, Rha and Glu of GRSDF, Man and Xyl of SHSDF, Man and Gal of LISDF, Rib of PISDF, Gala of GUSDF and WESDF were highlighted in the heatmap with a strong positive or negative correlative to the corresponding PLS-SDF. Among the six PSL-SDFs, GUSDF and WESDF were grouped together,



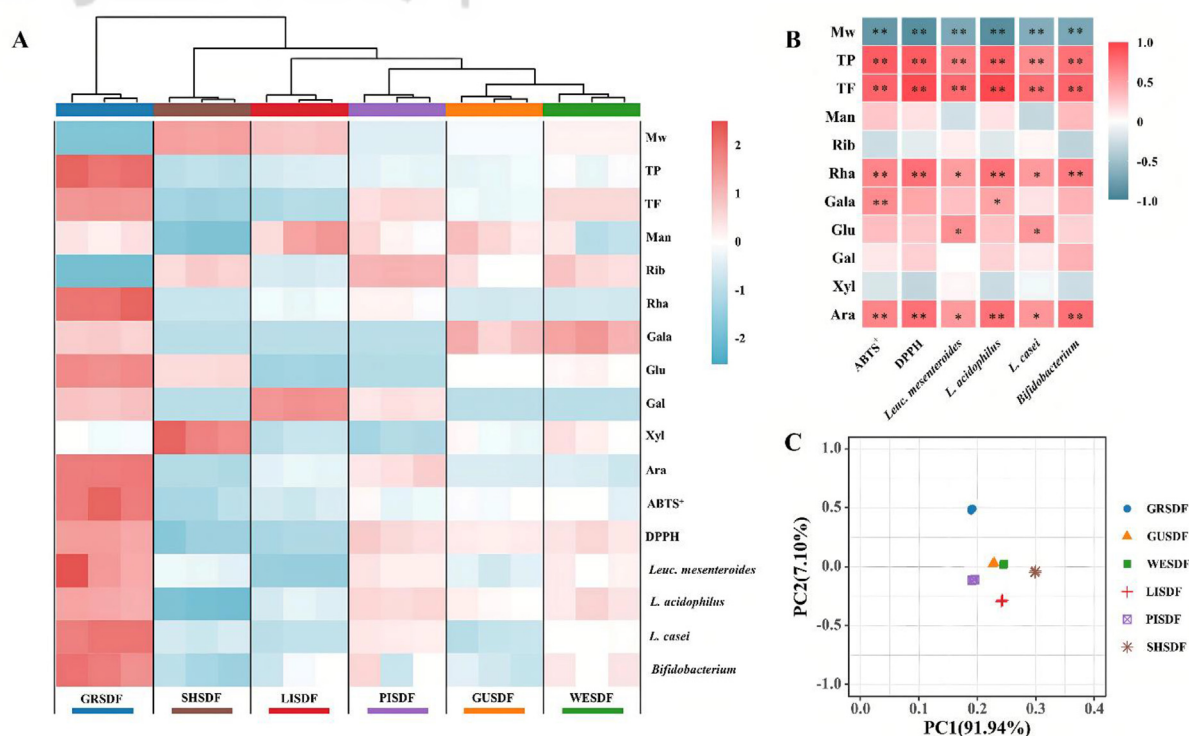


Fig. 6. Relationship of raw materials, structure and activity of different PSL-SDFs. (A) Heatmap representation; (B) correlation analysis; and (C) PCA analysis. \* $P < 0.05$ , \*\* $P < 0.01$ . GRSDF, GUSDF, WESDF, LISDF, PISDF, and SHSDF presented the PSL-SDF extracted from Grapefruit, Guanxi pomelo, Wendan pomelo, Liangping pomelo, Pingshan pomelo, and Shatian pomelo, respectively.

which was similar to the results of PCA analysis (Fig. 6C), showing that they shared similar structural property, bioactive compounds and activity functional characteristic. In contrast, GRSDF had the weakest association with other five PSL-SDFs, which was consistent with the results of the PCA analysis. Specifically, SHSDF and LISDF had negative correlations with ABTS<sup>+</sup> and DPPH free radical scavenging ability, while GRSDF showed the opposite situation. GRSDF was positively correlated with the promotion of probiotic growth, which was different from SHSDF and LISDF. These results might be due to the Mw and monosaccharide composition of GRSDF were quite different from those of SHSDF and LISDF [14]. According to previous studies, Mw, TP, TF, and monosaccharide composition of polysaccharides had great effects on their antioxidant and probiotic growth promotion capacities [39,48]. Hence, the Mw, TP, TF, and monosaccharide composition of PLS-SDFs were further investigated in relation to antioxidant capacity and probiotic growth promotion ability. As depicted in Fig. 6B, Mw was negatively related to the antioxidant and probiotic growth promotion capacities of PLS-SDFs ( $P < 0.01$ ), which was similar with the results of section 3.1 and 3.10. The increase in Mw raised the viscosity of the polysaccharide,

leading to an increase in the mass transfer resistance of the polysaccharides, which made it difficult for microorganisms to utilize the polysaccharides [47]. Moreover, low Mw polysaccharides were believed to have more hydroxyl terminals to eliminate free radicals. Fig. 6B exhibited that TP and TF had positive relationship with antioxidant and probiotic growth-promoting abilities ( $P < 0.01$ ), which was similar with a previous study [39]. In addition, the functional characteristics of PLS-SDFs were also impacted by their monosaccharide compositions. As shown in Fig. 6B, Rha and Ara contents of PSL-SDFs were positively correlated to their antioxidant and probiotic growth-promoting ability. Gala showed significantly positive correlation with the ABTS<sup>+</sup> free radical scavenging ability ( $P < 0.01$ ). Gala and Glu displayed positive relationship with the growth of *L. acidophilus*, *L. mesenteroides* and *L. casei* ( $P < 0.05$ ). Above results suggested that GRSDF exhibited better antioxidant and probiotic growth-promoting activities than other PSL-SDFs, which could be selected for further analysis.

#### 4. Conclusions

In the present study, results revealed that the varieties of pomelo had a great impact on the

physicochemical properties (Ash, fat, protein, TP and TF) of PSL-SDF. The Mw of all PSL-SDFs were in the range of 124.81–302.28 kDa. Moreover, SDFs isolated from different pomelo peel spongy layers displayed good performance in SC, WHC, OHC, antioxidant activities, resistance to gastric digestion, and probiotic growth-promoting ability. Indeed, correlation analysis showed that the multiple beneficial effects of PSL-SDFs were markedly associated with their Mw and the contents of TP, TF, Rha, Gala, Gluc and Ara. Compared with other PSL-SDFs, GRSDf showed better physicochemical and functional properties. The findings of this study suggested that these six PSL-SDFs had good physicochemical and functional characteristics, especially GRSDf, which had the potential to be

used as an additive in functional foods or health products.

### Conflict of interest

There is no conflict to declare.

### Acknowledgements

This study was funded by the Research and development program in key areas of Guangdong province (No. 2022B0202020003), Research Group Construction Project of Guangdong Academy of Agricultural Sciences (No. 202109TD), Special Fund for Scientific Innovation Strategy-construction of High-level Academy of Agricultural Science (No. R2020QD-033).

## Appendix A. Supplementary materials

Table 1. Detailed information on 6 varieties of pomelo.

Pomelo Sample	Location	Characteristic	Company
Grapefruit	Zhejiang, China	Grapefruit fruit shape is oblate to spherical, smaller than ordinary pomelo, the heart of the fruit is full, both bitter and numb tongue flavor, few or no seeds, multi-embryo, ripe in mid-October.	Anqin Fruit and Vegetable Specialized Cooperative
Guanxi pomelo	Fujian, China	Guanxi Pomelo's thin skin, no nucleus, juicy, known as "the crown of the pomelo", storage resistance, mature in late October.	Pomelo Town Food Co., Ltd.
Wendan pomelo	Zhejiang, China	Wendanyu pomelo fruit shape flat round, thick skin, few seeds, is a medicinal and dietary fruit, generally produced in early October.	Lynian Agricultural Technology Co., Ltd
Liangping pomelo	Chongqing, China	Liangping pomelo is a flat round fruit, the top of the fruit is nearly flat, the base is slightly narrow and rounded, the skin is thin and smooth, is China's pomelo pomelo representative varieties of flat top type pomelo, commonly known as "medicine pomelo", generally ripe at the end of October.	Chongqing Zhuolong E-commerce Co., Ltd
Pingshan pomelo	Fujian, China	Pingshan pomelo is oval in shape, both shoulders are cut, the top of the fruit is nearly flat, and there is a convex rib at the tip, sweet and less acidic flavor, juicy, resistant to storage and transportation, generally produced in early to mid-September, is more precocious pomelo varieties.	Pomelo Town Food Co., Ltd.
Shatian pomelo	Guangdong, China	Shatian pomelo is pear-shaped or gourd-shaped, the top of the fruit is slightly flat, there are obvious rings and radial grooves, the tip is narrow and prolonged in the shape of a neck, crisp and tender flesh, sweet flavor and juice, is the most widely planted pomelo varieties in China, usually produced in late October.	Meizhou Meixian Fuxinyuan Fruit Specialized Cooperative Society

Table 2. Thermal stability of different PSL-SDFs.

		T <sub>set</sub> (°C)	T <sub>peak</sub> (°C)	T <sub>end</sub> (°C)	Δ H (J/g)
GRSDF	First phase peak	58.23 ± 0.29 <sup>a</sup>	90.9 ± 0.17 <sup>a</sup>	118.37 ± 0.46 <sup>c</sup>	−210.5 ± 1.73 <sup>c</sup>
	Second phase peak	193.83 ± 0.92 <sup>d</sup>	214.73 ± 0.58 <sup>c</sup>	227.43 ± 0.06 <sup>b</sup>	24.41 ± 0.13 <sup>c</sup>
GUSDF	First phase peak	59.37 ± 0.06 <sup>a</sup>	87.5 ± 1.04 <sup>b</sup>	150.00 ± 0.35 <sup>a</sup>	−163.23 ± 0.64 <sup>d</sup>
	Second phase peak	216.83 ± 0.98 <sup>ab</sup>	224.03 ± 1.33 <sup>a</sup>	230.10 ± 1.39 <sup>a</sup>	−40.78 ± 1.25 <sup>b</sup>
WESDF	First phase peak	30.43 ± 0.46 <sup>c</sup>	67.7 ± 1.91 <sup>d</sup>	129.63 ± 0.64 <sup>b</sup>	−215.43 ± 2.66 <sup>b</sup>
	Second phase peak	215.10 ± 0.35 <sup>b</sup>	219.40 ± 0.17 <sup>b</sup>	225.13 ± 0.06 <sup>d</sup>	−2.73 ± 0.43 <sup>f</sup>
LISDF	First phase peak	56.13 ± 0.46 <sup>b</sup>	88.03 ± 1.62 <sup>b</sup>	115.67 ± 0.98 <sup>d</sup>	−120.2 ± 1.39 <sup>f</sup>
	Second phase peak	212.47 ± 1.50 <sup>c</sup>	222.6 ± 1.04 <sup>a</sup>	230.4 ± 1.04 <sup>a</sup>	−21.56 ± 1.59 <sup>e</sup>
PISDF	First phase peak	19.13 ± 0.20 <sup>d</sup>	74.57 ± 0.98 <sup>c</sup>	97.53 ± 0.58 <sup>e</sup>	−270.5 ± 1.91 <sup>a</sup>
	Second phase peak	192.53 ± 1.50 <sup>d</sup>	213.77 ± 0.40 <sup>c</sup>	225.83 ± 0.58 <sup>ab</sup>	22.21 ± 0.54 <sup>d</sup>
SHSDF	First phase peak	30.00 ± 0.35 <sup>c</sup>	57.70 ± 1.56 <sup>e</sup>	77.06 ± 0.92 <sup>f</sup>	−133.6 ± 1.73 <sup>e</sup>
	Second phase peak	217.53 ± 1.09 <sup>a</sup>	222.00 ± 2.25 <sup>a</sup>	230.57 ± 1.50 <sup>a</sup>	−45.16 ± 1.35 <sup>a</sup>

## References

- Turner ND, Lupton JR. Dietary fiber. *Adv Nutr* 2021;12:2553–5.
- Wang X, Geng X, Egashira Y, Sanada H. Purification and characterization of a Feruloyl esterase from the intestinal bacterium *Lactobacillus acidophilus*. *Appl Environ Microbiol* 2004;70:2367–72.
- Yu J, Fu Y, Deng Z, Fan Y, Li H. Effects of soluble dietary fiber from soybean residue fermented by *Neurospora crassa* on the intestinal flora in rats. *Food Funct* 2020;11:7433–45.
- Twarogowska A, Van Poucke C, Van Droogenbroeck B. Upcycling of Belgian endive (*Cichorium intybus* var. *foliosum*) by-products. Chemical composition and functional properties of dietary fibre root powders. *Food Chem* 2020;332:127444.
- Fuso A, Viscusi P, Righetti L, Pedrazzani C, Rosso G, Manera I, et al. Hazelnut (*Corylus avellana* L.) shells as a potential source of dietary fibre: impact of hydrothermal treatment temperature on fibre structure and degradation compounds. *J Sci Food Agric* 2023;103:7569–79.
- Perez-Pirotto C, Cozzano S, Hernando I, Arcia P. Different green extraction technologies for soluble dietary fibre extraction from orange by-product. *Int J Food Sci Technol* 2023;58:2042–9.
- Campos DA, Coscueta ER, Vilas-Boas AA, Silva S, Teixeira JA, Pastrana LM, et al. Impact of functional flours from pineapple by-products on human intestinal microbiota. *J Funct Foods* 2020;67:103830.
- Xiao L, Ye F, Zhou Y, Zhao G. Utilization of pomelo peels to manufacture value-added products: a review. *Food Chem* 2021;351:129247.
- Gupta AK, Koch P, Mishra P. Optimization of debittering and deacidification parameters for Pomelo juice and assessment of juice quality. *J Food Sci Technol* 2020;57:4726–32.
- Chen L, Jiang X, Sun Y, Gan D, Liu W, Wu Y, et al. Composite optimization and characterization of dietary fiber-based edible packaging film reinforced by nanocellulose from grapefruit peel pomace. *Int J Biol Macromol* 2023;253:127655.
- Qin X, Dong X, Tang J, Chen Y, Xie J, Cheng Y, et al. Comparative analysis of dietary fibers from grapefruit peel prepared by ultrafine grinding: structural properties, adsorption capacities, in vitro prebiotic activities. *Food Biosci* 2023;56:103163.
- Gan J, Huang Z, Yu Q, Peng G, Chen Y, Xie J, et al. Microwave assisted extraction with three modifications on structural and functional properties of soluble dietary fibers from grapefruit peel. *Food Hydrocoll* 2020;101:105549.
- Gamonpilas C, Buathongjan C, Kirdsawasd T, Rattanaprasert M, Klomtun M, Phonsatta N, et al. Pomelo pectin and fiber: some perspectives and applications in food industry. *Food Hydrocoll* 2021;120:106981.
- Deng M, Lin Y, Dong L, Jia X, Shen Y, Liu L, et al. Physicochemical and functional properties of dietary fiber from pummelo (*Citrus grandis* L. Osbeck) and grapefruit (*Citrus paradisi* Mcfad) cultivars. *Food Biosci* 2021;40:100890.
- Liu J, Wang Z, Wang Z, Hao Y, Wang Y, Yang Z, et al. Physicochemical and functional properties of soluble dietary fiber from different colored quinoa varieties (*Chenopodium quinoa* Willd). *J Cereal Sci* 2020;95:103045.
- Hu Y, Hu J, Li J, Wang J, Zhang X, Wu X, et al. Physicochemical characteristics and biological activities of soluble dietary fibers isolated from the leaves of different quinoa cultivars. *Food Res Int* 2023;163:112166.
- Kaur S, Panesar PS, Chopra HK. Extraction of dietary fiber from kinnow (*Citrus reticulata*) peels using sequential ultrasonic and enzymatic treatments and its application in development of cookies. *Food Biosci* 2023;54:102891.
- Yang Y, Wang Z, Hu D, Xiao K, Wu JY. Efficient extraction of pectin from sisal waste by combined enzymatic and ultrasonic process. *Food Hydrocolloids* 2018;79:189–96.
- AOAC. Official method of analysis of AOAC International. 18th ed. 2005. Chapter 930.909.
- Cao X, Zhang Y, Zhang F, Wang Y, Yi J, Liao X. Effects of high hydrostatic pressure on enzymes, phenolic compounds, anthocyanins, polymeric color and color of strawberry pulps. *J Sci Food Agric* 2011;91:877–85.
- Martínez R, Torres P, Meneses MA, Figueroa JG, Pérez-Álvarez JA, Viuda-Martos M. Chemical, technological and in vitro antioxidant properties of mango, guava, pineapple and passion fruit dietary fibre concentrate. *Food Chem* 2012;135:1520–6.
- Huang J, Zhao C, Li J, Hussain S, Yan S, Wang Q. Structural and physicochemical properties of pectin-rich dietary fiber prepared from citrus peel. *Food Hydrocoll* 2021;110:106140.
- Moczowska M, Karp S, Niu Y, Kurek MA. Enzymatic, enzymatic-ultrasonic and alkaline extraction of soluble dietary fibre from flaxseed – a physicochemical approach. *Food Hydrocoll* 2019;90:105–12.
- Slavov A, Panchev I, Kovacheva D, Vasileva I. Physicochemical characterization of water-soluble pectic extracts from *Rosa damascena*, *Calendula officinalis* and *Matricaria chamomilla* wastes. *Food Hydrocoll* 2016;61:469–76.
- Wei C, Ge Y, Liu D, Zhao S, Wei M, Jiliu J, et al. Effects of high-temperature, high-pressure, and ultrasonic treatment on the physicochemical properties and structure of soluble dietary fibers of millet bran. *Front Nutr* 2022;8.
- Wang S, Fang Y, Xu Y, Zhu B, Piao J, Zhu L, et al. The effects of different extraction methods on physicochemical, functional and physiological properties of soluble and insoluble dietary fiber from *Rubus chingii* Hu. fruits. *J Funct Foods* 2022;93:105081.

- [27] Hua M, Lu J, Qu D, Liu C, Zhang L, Li S, et al. Structure, physicochemical properties and adsorption function of insoluble dietary fiber from ginseng residue: a potential functional ingredient. *Food Chem* 2019;286:522–9.
- [28] Chen H, Zhao C, Li J, Hussain S, Yan S, Wang Q. Effects of extrusion on structural and physicochemical properties of soluble dietary fiber from nodes of lotus root. *LWT-Food Sci Technol* 2018;93:204–11.
- [29] Fathi M, Mohebbi M, Koocheki A. Introducing *Prunus cerasus* gum exudates: chemical structure, molecular weight, and rheological properties. *Food Hydrocoll* 2016;61:946–55.
- [30] Karaman E, Yölmaz E, Tuncel NB. Physicochemical, microstructural and functional characterization of dietary fibers extracted from lemon, orange and grapefruit seeds press meals. *Bioact* 2017;11:9–17.
- [31] Tan F, Yu Y, Xu YJ, Wu J, Xiao G, Hu T. Physicochemical properties and biological activities of litchi glycans with different molecular weight. *Int J Food Sci Technol* 2024;59: 105–19.
- [32] Chen B, Cai Y, Liu T, Huang L, Deng X, Zhao Q, et al. Improvements in physicochemical and emulsifying properties of insoluble soybean fiber by physical-chemical treatments. *Food Hydrocoll* 2019;93:167–75.
- [33] Ma M, Mu T. Effects of extraction methods and particle size distribution on the structural, physicochemical, and functional properties of dietary fiber from deoiled cumin. *Food Chem* 2016;194:237–46.
- [34] Jiang Y, Yin H, Zheng Y, Wang D, Liu Z, Deng Y, et al. Structure, physicochemical and bioactive properties of dietary fibers from *Akebia trifoliata* (Thunb.) Koidz. seeds using ultrasonication/shear emulsifying/microwave-assisted enzymatic extraction. *Food Res Int* 2020;136:109348.
- [35] Li Y, Yu Y, Wu J, Xu Y, Xiao G, Li L, et al. Comparison the structural, physicochemical, and prebiotic properties of litchi pomace dietary fibers before and after modification. *Foods* 2022;11:248.
- [36] Cheng L, Zhang X, Hong Y, Li Z, Li C, Gu Z. Characterisation of physicochemical and functional properties of soluble dietary fibre from potato pulp obtained by enzyme-assisted extraction. *Int J Biol Macromol* 2017;101:1004–11.
- [37] Garau MC, Simal S, Rosselló C, Femenia A. Effect of air-drying temperature on physico-chemical properties of dietary fibre and antioxidant capacity of orange (*Citrus aurantium* v. *Canoneta*) by-products. *Food Chem* 2007;104: 1014–24.
- [38] Wang Q, Luo J, Liu H, Brennan CS, Liu J, Zou X. Protective effects of the flavonoid fraction obtained from pomelo fruitlets through ultrasonic-associated microwave extraction against AAPH-induced erythrocyte hemolysis. *RSC Adv* 2019;9:16007–17.
- [39] Chen H, Xiong M, Bai T, Chen D, Zhang Q, Lin D, et al. Comparative study on the structure, physicochemical, and functional properties of dietary fiber extracts from quinoa and wheat. *LWT-Food Sci Technol* 2021;149:111816.
- [40] Huang H, Chen J, Chen Y, Xie J, Liu S, Sun N, et al. Modification of tea residue dietary fiber by high-temperature cooking assisted enzymatic method: structural, physicochemical and functional properties. *LWT-Food Sci Technol* 2021;145:111314.
- [41] Hu X, Xu F, Li J, Li J, Mo C, Zhao M, et al. Ultrasonic-assisted extraction of polysaccharides from coix seeds: optimization, purification, and in vitro digestibility. *Food Chem* 2022;374: 131636.
- [42] Wichienchot S, Jatupornpipat M, Rastall RA. Oligosaccharides of pitaya (dragon fruit) flesh and their prebiotic properties. *Food Chem* 2010;120:850–7.
- [43] Hu JL, Nie SP, Min FF, Xie MY. Artificial simulated saliva, gastric and intestinal digestion of polysaccharide from the seeds of *Plantago asiatica* L. *Carbohydr Polym* 2013;92:1143–50.
- [44] Chen C, Zhang B, Fu X, You LJ, Abbasi AM, Liu RH. The digestibility of mulberry fruit polysaccharides and its impact on lipolysis under simulated saliva, gastric and intestinal conditions. *Food Hydrocoll* 2016;58:171–8.
- [45] Xue Z, Chen Z, Gao X, Zhang M, Panichayupakaranant P, Chen H. Functional protection of different structure soluble dietary fibers from *Lentinus edodes* as effective delivery substrate for *Lactobacillus plantarum* LP90. *LWT-Food Sci Technol* 2021;136:110339.
- [46] Peng J, Bu Z, Ren H, He Q, Yu Y, Xu Y, et al. Physicochemical, structural, and functional properties of wampee (*Clausena lansium* (Lour.) Skeels) fruit peel pectin extracted with different organic acids. *Food Chem* 2022;386:132834.
- [47] Wang X, Huang M, Yang F, Sun H, Zhou X, Guo Y, et al. Rapeseed polysaccharides as prebiotics on growth and acidifying activity of probiotics in vitro. *Carbohydr Polym* 2015;125:232–40.
- [48] Gu Q, Gao X, Zhou Q, Li Y, Li G, Li P. Characterization of soluble dietary fiber from citrus peels (*Citrus unshiu*), and its antioxidant capacity and beneficial regulating effect on gut microbiota. *Int J Biol Macromol* 2023;246:125715.